IOP Publishing New J. Phys. 26 (2024) 073034 https://doi.org/10.1088/1367-2630/ad6283

New Journal of Physics
The open access journal at the forefront of physics

Deutsche Physikalische Gesellschaft DPG
IOP Institute of Physics

Published in partnership with: Deutsche Physikalische Gesellschaft and the Institute of Physics

OPEN ACCESS

RECEIVED
7 March 2024

REVISED
25 June 2024

ACCEPTED FOR PUBLICATION
12 July 2024

PUBLISHED
23 July 2024

PAPER

Efficient and reliable detection of nonlocal quantum correlations in continuous-variable and hybrid states via random measurements

Artur Barasiński[1,*], **Nazarii Sudak**[1] **and Jan Peřina Jr**[2]

[1] Institute of Theoretical Physics, University of Wroclaw, Plac Maxa Borna 9, 50-204 Wrocław, Poland
[2] Joint Laboratory of Optics of Palacký University and Institute of Physics of CAS, Faculty of Science, Palacký University, 17. listopadu 12, 771 46 Olomouc, Czech Republic
[*] Author to whom any correspondence should be addressed.

E-mail: artur.barasinski@uwr.edu.pl

Keywords: optical tests of quantum theory, hybrid quantum systems, non-gaussian quantum states, quantum correlations in quantum information, entanglement detection, nonlocality

Abstract

We investigate the violation of nonlocal realism using various entangled continues- and hybrid-variable states under dichotomic observables. In particular, we consider two cases of dichotomic observables (1) described by a pseudospin operator and (2) given in terms of the Wigner representation of the state in phase space, parity measurement and displacement operation. We address the recently proposed operational measure of nonlocality which describes the probability of local-realism violation under randomly sampled observables. We show the usefulness and limitations of the probability of local-realism violation for the detection of nonlocality. A simple procedure to detect such nonlocal correlations for randomly chosen settings with efficiencies of up to 100% is proposed. The practical advantage of applying random measurements that considerably lowers the experimental requirements is mentioned.

1. Introduction

One of the most remarkable features of quantum mechanics is that distant measurements can exhibit correlations being inconsistent with any locally-causal description [1]. Although this feature was initially thought to be evidence of the incompleteness of the quantum theory [2], there is nowadays the overwhelming experimental evidence that the nature is indeed nonlocal [3].

Nonlocality plays the central role in quantum-information science and has been recognized as an essential resource for quantum-information tasks [4] including quantum key distribution [5], communication complexity [6], randomness generation [7], and device-independent information processing [8, 9]. In particular, the presence of nonlocal correlations is widely used as a simple and strong device-independent test for certifying the presence of entanglement [10, 11]. However, nonlocal correlations are correlations of the measurement outcomes. As such, they are not solely a consequence of entanglement but they also depend upon the choice of the measurements.

Demonstrations of nonlocal correlations typically employ the carefully chosen measurements [12]. Moreover, such specific measurements depend on the analyzed state. This necessarily requires the spatially separated observers to share a complete reference frame that has to be well-aligned and also to have some knowledge about the exact shape of the quantum-state density matrix. To circumvent these requirements, the observers may use the correlated quantum systems to establish a shared reference frame and perform a complete state tomography. However, these approaches are resource-intensive, since they require the use of many entangled quantum states.

Recently, it has been shown that such methods are not required to demonstrate the violation of the Bell inequality. Contrary to that, one can analyze nonlocal correlations of complex states using the probability that random measurements generate nonlocal statistics. The probability of local-realism violation under

random measurements, proposed in [13, 14], has gained considerable attention as an operational measure of the nonclassicality of a quantum state [15]. It has been demonstrated both numerically [13, 16, 17] and analytically [18] that for N spatially separated observers the most choices of the measurement lead to nonlocal correlations between the measurement outcomes. In other words, the probability of local-realism violation under random measurements approaches 1 as N increases. Furthermore, in [18] it has been proven that this quantifier obeys certain natural properties and expectations for an operational measure of nonclassicality, e.g. invariance under local unitary operations. The probability of violation can also be easily implemented experimentally. The error arising from this approach is comparable to the usual measurement errors [17, 19]. The probability of violation can also be used to establish the degree of entanglement of a quantum state [20].

However, all these studies assume discrete entangled states. A question naturally arises about the usefulness of the probability of violation for more general quantum systems described, e.g. by the continuous variable (CV) states. Here, Chen *et al* [21] have studied the Bell inequality using the pseudospin formalism which, together with the parity operator, closes an SU(2) algebra. Such approach yields the maximal violation of the Clauser, Horne, Shimony, and Holt (CHSH) [22] inequality, and so one may expect that the probability of violation for two-mode CV states derived using the pseudospin formalism behaves similarly as that of the entangled qubit states. However, the pseudospin approach is not implementable easily experimentally.

In contrast, Banaszek and Wódkiewicz (BW) have studied the Bell inequality for CV states using the Wigner-function representation in phase space, the derived parity measurements and displacement operation [23, 24]. Since the parity operator is a dichotomic observable, BW were able to construct a CHSH-type inequality which is especially experimentally interesting. The violations of such Bell inequality can be demonstrated using photon detection, either photon-number-resolving measurements or photon presence measurements [25, 26]. Successful experimental implementations of parity measurements via photon-number-resolving detection can be found in [27–29]. We note that the BW approach, unfortunately, does not always lead to the maximal violation of the CHSH inequality [30], even when its generalized version is considered [26].

In this paper, we tackle this problem by considering CV and hybrid quantum systems and applying both the pseudo-spin approach and the approach based on the Wigner function to arrive at the probability of local-realism violation. In section 2, the used methods are described and discussed. Results obtained for both approaches and different states are analyzed in section 3. Conclusions are drawn in section 4.

2. Description of the method

2.1. Bell nonlocality and its quantification

Let us consider a family of Bell-CHSH relations (equivalent under permutation of parties, inputs, and outputs) given by

$$\mathcal{B}_{\mathrm{CHSH}} = C(\omega_A,\omega_B) + C(\omega_A,\omega_B')\, C(\omega_A',\omega_B) - C(\omega_A',\omega_B'),$$

where $C(\omega_A,\omega_B)$ is the correlation function between parties A and B when the measurements are set for parameters ω_A and ω_B. Then the local realistic theorem imposes the following inequality

$$|\langle \mathcal{B}_{\mathrm{CHSH}} \rangle| \leqslant 2, \tag{1}$$

where $\langle \mathcal{B}_{\mathrm{CHSH}} \rangle$ stands for the expectation value of $\mathcal{B}_{\mathrm{CHSH}}$ with respect to a given quantum state.

If for given settings $\Omega = \{\omega_A,\omega_A',\omega_B,\omega_B'\}$ the Bell relation does not obey the inequality (1), the correlations between the measurements outcomes are said to be Bell nonlocal. Note that nonlocal correlations of a bipartite state with two measurements and two outcomes per party are fully characterized by the CHSH inequality, assuming the freedom in relabeling all measurement settings and/or outcomes and/or parties [31].

For a given Bell scenario, the values of Ω settings which lead to the violation of local realistic description solely depend on the analyzed state. So it is necessary to know the form of the quantum-state density matrix. Especially, when the degree of violation of the Bell inequality is used as a measure of nonlocality.

To tackle this problem, another may how to quantify nonlocal correlations of complex states was proposed in [13, 14] by introducing the probability of local-realism violation under random measurements. It is defined as [13, 14]

$$\mathcal{P}_{\mathrm{V}}(\rho) = \int f(\rho,\Omega)\, \mathrm{d}\Omega, \tag{2}$$

where ρ stands for the quantum-state density matrix and we integrate over the space of measurement parameters $\Omega = \{\omega_A, \omega_A', \omega_B, \omega_B'\}$ that vary within the Bell scenario according to the Haar measure. The function $f(\rho, \Omega)$ attains one of two possible values

$$f(\rho,\Omega) = \begin{cases} 1 & \text{if settings lead to the violation} \\ & \text{of local realism,} \\ 0, & \text{otherwise.} \end{cases}$$

For the CHSH scenario and maximally entangled two-qubit states, the probability of violation takes its maximal value of $\mathcal{P}_{\max} = 2(\pi - 3) \approx 28.3\%$ [13].

2.2. Correlation function for CV states

For CV systems, there are two well-known definitions of the correlation function $C(\omega_A, \omega_B)$ based either on the pseudospin or the Wigner-function formalism.

Pseudospin formalism For a single-mode light field the following pseudospin operators $\hat{\mathbf{s}} = (\hat{s}_x, \hat{s}_y, \hat{s}_z)$ are introduced [21] for a nonlocality test:

$$\begin{aligned} \hat{s}_z &= \sum_{n=0}^{\infty} \left(|2n+1\rangle\langle 2n+1| - |2n\rangle\langle 2n| \right), \\ \hat{s}_{\pm} &= \left(\hat{s}_x \pm \mathrm{i}\hat{s}_y \right)/2, \\ \hat{s}_- &= (\hat{s}_+)^{\dagger} = \sum_{n=0}^{\infty} |2n\rangle\langle 2n+1|, \end{aligned} \tag{3}$$

and $|n\rangle$ denote the usual Fock states. Within this scheme, the correlation function reads $C(\mathbf{a}, \mathbf{b}) = \langle \mathbf{a}\cdot\hat{\mathbf{s}}_1 \otimes \mathbf{b}\cdot\hat{\mathbf{s}}_2 \rangle$, where $\mathbf{a}$ and $\mathbf{b}$ denote the unit vectors, and $\hat{\mathbf{s}}_j$ is the pseudospin operator for jth party ($j = 1, 2$). Each unit vector can be characterized by a pair of angles $\{\theta, \phi\}$. Then the scalar product is given by

$$\mathbf{a}\cdot\hat{\mathbf{s}}_1 = \hat{s}_z \cos\theta_a + \sin\theta_a \left[\exp(\mathrm{i}\phi_a)\hat{s}_- + \exp(-\mathrm{i}\phi_a)\hat{s}_+ \right], \tag{4}$$

and similar expressions hold for $\mathbf{b}\cdot\hat{\mathbf{s}}_2$. The relation (1) in then given as

$$\mathcal{B}_S = (\mathbf{a}\cdot\hat{\mathbf{s}}_1)\otimes(\mathbf{b}\cdot\hat{\mathbf{s}}_2) + (\mathbf{a}'\cdot\hat{\mathbf{s}}_1)\otimes(\mathbf{b}\cdot\hat{\mathbf{s}}_2) + (\mathbf{a}\cdot\hat{\mathbf{s}}_1)\otimes\left(\mathbf{b}'\cdot\hat{\mathbf{s}}_2\right) - (\mathbf{a}'\cdot\hat{\mathbf{s}}_1)\otimes\left(\mathbf{b}'\cdot\hat{\mathbf{s}}_2\right). \tag{5}$$

It is straightforward to see that, within the pseudospin formalism, the space of measurement parameters Ω in (2) is spanned by the set of angles $\{\theta_a, \phi_a, \ldots, \theta_b', \phi_b'\}$ that characterize the unit vectors $\mathbf{a}$, $\mathbf{a}'$, $\mathbf{b}$, $\mathbf{b}'$.

Wigner-function formalism: First, let us recall the definition of the Wigner function of a bipartite quantum state ρ [32, 33]:

$$W(\omega_A, \omega_B) = \mathrm{Tr}\left[\rho \hat{\Delta}_A(\omega_A) \otimes \hat{\Delta}_B(\omega_B) \right], \tag{6}$$

where ω_A (ω_B) denotes the set of measurement parameters for party A (B), similarly as before; $\Delta_A(\omega_A)$ ($\Delta_B(\omega_B)$) is the kernel operator corresponding to party A (B). In particular, when ρ describes a bipartite CV quantum system the kernel operator takes the well-known form [32]

$$\hat{\Delta}_A(\omega_A) \equiv \hat{\Delta}(\alpha) = \frac{2}{\pi}\hat{D}(\alpha)\hat{\Pi}\hat{D}^{\dagger}(\alpha), \tag{7}$$

where $\hat{D}(\alpha) = \exp[\alpha\hat{a}^{\dagger} - \alpha^*\hat{a}]$ is the displacement operator [32], $\hat{\Pi} = \exp(\mathrm{i}\pi\hat{a}^{\dagger}\hat{a})$ denoted the bosonic parity operator, and $\hat{a}$ ($\hat{a}^{\dagger}$) stands for the annihilation (creation) bosonic operator. Similarly one defines $\hat{\Delta}_B(\omega_B) = \hat{\Delta}(\beta)$ for party B.

Following BW [23, 24], we consider the optical experiment when the detectors are capable of resolving the number of absorbed photons. In this case, the Bell events ± 1 can be assigned to the fact whether an even or an odd number of photons has been registered. Consequently, the correlation function $C(\alpha, \beta) = \langle \hat{D}(\alpha)\hat{\Pi}\hat{D}^{\dagger}(\alpha) \otimes \hat{D}(\beta)\hat{\Pi}\hat{D}^{\dagger}(\beta) \rangle$ [23, 24]. Based on equation (6) one can write

$$C(\alpha,\beta) = \frac{\pi^2}{4}\langle \hat{\Delta}(\alpha)\otimes\hat{\Delta}(\beta)\rangle = \frac{\pi^2}{4}W(\alpha,\beta), \tag{8}$$

where $W(\alpha, \beta)$ represents the Wigner function of the analyzed CV quantum state. The Bell parameter is then defined as

$$\mathcal{B}_W = \frac{\pi^2}{4}\left(W(\alpha,\beta) + W(\alpha,\beta') + W(\alpha',\beta) - W(\alpha',\beta') \right), \tag{9}$$

and the space of measurement parameters Ω is spanned by the complex field amplitudes $\{\alpha,\alpha',\beta,\beta'\}$. The general expression is referred to as the generalized BW formalism [26], while in the original BW approach [23, 24] two of the four parameters are assumed to be zero, namely $\alpha=\beta=0$.

Finally, it is important to note that the violation of the Bell inequality (9) does not necessarily imply the negativity of the Wigner function for the analyzed state. There are well-documented cases of states with a positive Wigner function that still violate the inequality (9), and conversely, instances where the Bell inequality is not violated despite the Wigner function not being positive definite [23, 24]. This discrepancy arises because the Wigner representation of the parity operator does not correspond to a bounded reality, as it reflects the dichotomic outcome of the measurement.

2.3. Bell inequality for hybrid states

Let us now introduce the CHSH-like inequality for quantum states that involve both discrete and CVs. In particular, for a hybrid bipartite state with density matrix ρ_H composed of a bosonic field (party A) and a qubit (party B) one can arrive at the pseudospin formalism by replacing $\sum_{n=0}^{\infty}\to\sum_{n=0}^{1}$ in equation (3) concerning the qubit part.

On the other hand, the Wigner-function formalism is introduced based on equations (6) and (7) together with the formula

$$\hat{\Delta}_B(\omega_B)\equiv\hat{\Delta}_q(\theta,\phi)=\frac{1}{2}\hat{U}(\theta,\phi)\,\hat{\Pi}_q\hat{U}^{\dagger}(\theta,\phi), \tag{10}$$

where $\hat{U}(\theta,\phi)$ is the unitary SU(2) rotation operator and $\Pi_q=\mathbb{1}_2-\sqrt{3}\hat{\sigma}_3$ denotes the parity operator of the single qubit with the Pauli operators σ_3 [33]. Consequently, the Wigner function of ρ_H reads as

$$W(\alpha,\theta,\phi)=\frac{1}{2}W_A(\alpha)-\frac{\sqrt{3}}{\pi}C(\alpha,\theta,\phi), \tag{11}$$

where $W_A(\alpha)=\mathrm{Tr}[\rho_A\hat{\Delta}(\alpha)]$ denotes the Wigner function of the reduced bosonic state $\rho_A=\mathrm{Tr}_B[\rho_H]$. We introduce a new correlation function

$$C(\alpha,\theta,\phi)=\mathrm{Tr}\left[\rho_H\hat{D}(\alpha)\,\hat{\Pi}\,\hat{D}^{\dagger}(\alpha)\otimes U(\theta,\phi)\,\hat{\sigma}_3\hat{U}^{\dagger}(\theta,\phi)\right]. \tag{12}$$

It is important to note that $U(\theta,\phi)\hat{\sigma}_3\hat{U}^{\dagger}(\theta,\phi)$ can be replaced by $\mathbf{b}\cdot\hat{\boldsymbol{\sigma}}$, where $\mathbf{b}$ is the unit vector and $\hat{\boldsymbol{\sigma}}=(\hat{\sigma}_1,\hat{\sigma}_2,\hat{\sigma}_3)$ using the Pauli operators σ_i, $i=1,2,3$ (c.f. the psudospin formalism). Finally, the Bell parameter $\mathcal{B}_H$ for the hybrid state ρ_H is defined as

$$\mathcal{B}_H=\frac{\pi}{\sqrt{3}}\left(W(\alpha,\theta,\phi)+W(\alpha,\theta',\phi')+W(\alpha',\theta,\phi)-W(\alpha',\theta',\phi')-W_A(\alpha)\right). \tag{13}$$

3. Numerical results

In this section, we investigate probabilities $\mathcal{P}_{\mathrm{V}}$ of violation for several important states applying the pseudospin formalism and the Wigner-function formalism. Specifically, we examine the properties of several bipartite states that are often considered as nonclassical resources:

- Two-mode squeezed state (TMSS)

$$|\mathrm{TMSS}\rangle=\sum_{n=0}^{\infty}\frac{(\tanh r)^n}{\cosh r}|n\rangle|n\rangle, \tag{14}$$

  where $|n\rangle$ are the usual Fock states and r is the squeezing parameter.
- Singlet-like entangled coherent state (ECS1)

$$|\mathrm{ECS}_1\rangle=\mathcal{N}_1^{-1}\left(|\gamma\rangle|-\gamma\rangle-|-\gamma\rangle|\gamma\rangle\right), \tag{15}$$

  where $\mathcal{N}_1=\sqrt{2[1-\exp(-4\gamma)]}$ and $|\gamma\rangle$ denotes the coherent state with amplitude $\gamma\neq0$. Without the loss of generality) we assume $\gamma\in\mathbb{R}^+$.
- Triplet-like entangled coherent state (ECS2)

$$|\mathrm{ECS}_2\rangle=\mathcal{N}_2^{-1}\left(|\gamma\rangle|\gamma\rangle+|-\gamma\rangle|-\gamma\rangle\right), \tag{16}$$

  where $\mathcal{N}_2=\sqrt{2[1+\exp(-4\gamma)]}$, $\gamma\neq0$, and $\gamma\in\mathbb{R}^+$ similarly as before.

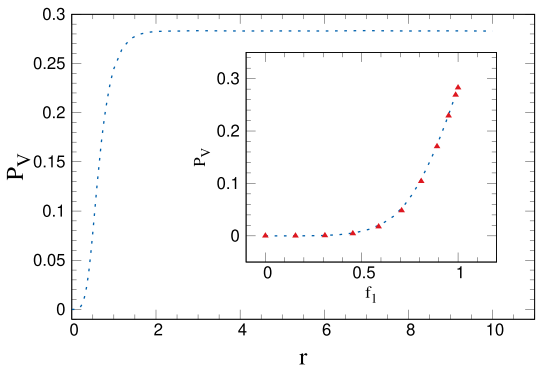

Figure 1. Probability $\mathcal{P}_V$ of violation for TMSS as a function of squeezing parameter r. The inset shows mutual relations between $\mathcal{P}_V$(TMSS) (plain dotted curve) and $\mathcal{P}_V(Q)$ (dotted curve with triangles) vs. function f_1, where $f_1(r) = \tanh(2r)$ for TMSS and $f_1(\theta) = \sin(2\theta)$ for two-qubit state Q defined as $|Q\rangle = \cos\theta|0\rangle|0\rangle + \sin\theta|1\rangle|1\rangle$.

- Hybrid qubit-Schrödinger cat state

$$|H\rangle = \frac{1}{\sqrt{2}}\left(|0\rangle|\gamma\rangle + |1\rangle|-\gamma\rangle\right), \tag{17}$$

where $\gamma \neq 0$ and $\gamma \in \mathbb{R}^+$.

3.1. Pseudospin operators

In the pseudospin formalism, the space of measurement parameters Ω is parameterized by the angles determining the unit vectors **a**, **a**′, etc. To generate their values according to the Haar measure, we apply the method described in [34]. Specifically, the values of angles ϕ_i, $i \in \{a, a', b, b'\}$, are sampled independently and uniformly in the ranges $\langle 0, 2\pi)$. Similarly, the values of angles $\theta_i = \arcsin(\xi_i^{1/2})$ are derived from auxiliary random variables ξ_i distributed uniformly in the interval $0 \leqslant \xi_i < 1$ for $i \in \{a, a', b, b'\}$. The number of measurement settings was chosen to ensure that results remained consistent up to the fifth decimal place, typically requiring between 10^8 and 10^9 settings. The numerical analysis has resulted in the following observations:

(a) For the TMSS the correlation function $C(\theta_a, \phi_a, \theta_b, \phi_b)$ takes the form

$$C(\theta_a, \phi_a, \theta_b, \phi_b) = \cos\theta_a \cos\theta_b + f_1(r) \sin\theta_a \sin\theta_b \cos(\phi_a + \phi_b), \tag{18}$$

where $f_1(r) = \tanh(2r)$. Substituting this equation to the CHSH expression the operator $\mathcal{B}_S$ given in equation (5) is determined and plotted in figure 1. The probability $\mathcal{P}_V$ of violation increases as the value of squeezing parameter r grows and reaches its maximum value $\mathcal{P}_{\max}$ when $r \to \infty$. This reflects the fact that the TMSS becomes the maximally entangled state in the $(2 \times 2)-$Hilbert space when $r \to \infty$ [21]. We note that $\mathcal{P}_V$ is close to $\mathcal{P}_{\max}$ already for $r > 2$. Also the correlation function in equation (18) is identical to that of the two-qubit state $|Q\rangle = \cos\theta|0\rangle|0\rangle + \sin\theta|1\rangle|1\rangle$ provided that $f_1(r)$ is replaced by $\sin(2\theta)$ (see the inset in figure 1). This means that $r \to \infty$ is equivalent to $\theta \to \pi/4$.

(b) For the singlet-like state ECS1 the correlation function is given by [26]

$$C(\theta_a, \phi_a, \theta_b, \phi_b) = -\cos\theta_a \cos\theta_b - f_2(\gamma) \sin\theta_a \sin\theta_b \cos(\phi_a - \phi_b), \tag{19}$$

where

$$f_2(\gamma) = 2\,\mathrm{csch}\left(2\gamma^2\right)\left(\sum_{n=0}^{\infty} \frac{\gamma^{4n+1}}{\sqrt{(2n)!\,(2n+1)!}}\right)^2 \tag{20}$$

and csch stands for the hyperbolic cosecant function. In this case, the probability of violation $\mathcal{P}_V$ approaches the maximum value $\mathcal{P}_{\max}$ in two extreme cases: $\gamma \to 0$ and $\gamma \to \infty$ (see figure 2), despite the ECS1 is maximally entangled in the $(2 \times 2)-$Hilbert space (but not in the infinite-dimensional Hilbert space) in the entire range of γ. For small γ, the local minimum of $\mathcal{P}_V$ is observed. It is because the pseudospin formalism for CV is not completely identical to that of a two-qubit system when a qubit is composed of two orthogonal even and odd macroscopic coherent states [35]. Specifically, the ECS1 can be rewritten in the $(2 \times 2)-$

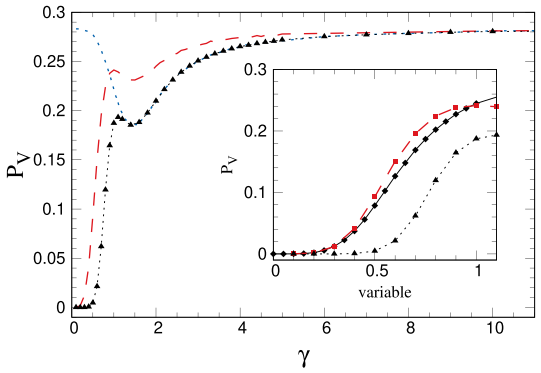

Figure 2. Probability $\mathcal{P}_V$ of violation for ECS1 (plain dotted line), ECS2 (dotted curve with triangles), and HS (plain dashed curve) as a function of coherent amplitude γ. The inset shows mutual relations between $\mathcal{P}_V$(TMSS) (solid curve with diamonds), $\mathcal{P}_V(\mathrm{ECS}_2)$ (dotted curve with triangles), and $\mathcal{P}_V(H)$ (dashed curve with squares) as a function of squeezing parameter r (TMSS) and coherent amplitude γ (ECS2 and HS).

Hilbert space based on the new orthonormal basis for coherent fields containing the even and odd coherent states $|\pm\rangle = \mathcal{N}_\pm^{-1}(|\gamma\rangle \pm |-\gamma\rangle)$, where $\mathcal{N}_\pm = \sqrt{2[1 \pm \exp(-2\gamma^2)]}$. The role of the base states $|\pm\rangle$ in forming ECS1 is completely interchangeable only for $\gamma \to 0$ and $\gamma \to \infty$. The same effect is observed when the strength of violation is analyzed [26]. Moreover, the minimum of $\mathcal{P}_V$ is reached for the same γ that implies the minimum of the strength of violation.

(c) For the triplet-like state ECS2 the correlation function takes the form written in equation (18) with function $f_1(r)$ replaced by function $f_3(\gamma)$,

$$f_3(\gamma) = \frac{4\exp(2\gamma^2)}{1+\exp(4\gamma^2)}\left(\sum_{n=0}^{\infty}\frac{\gamma^{4n+1}}{\sqrt{(2n)!\,(2n+1)!}}\right)^2. \tag{21}$$

In contrast to the singlet-like ECS1, the probability $\mathcal{P}_V$ of violation for ECS2 approaches the maximum value only when $\gamma \to \infty$. For $\gamma \to 0 \mathcal{P}_V \to 0$ is observed (figure 2). This is because the ECS2 becomes separable in the (2×2) Hilbert space for $\gamma \to 0$. Using the even and odd coherent states, the ECS2 is expressed as

$$|\mathrm{ECS}_2\rangle = \frac{\mathcal{N}_+^2}{2\mathcal{N}_2}|+\rangle|+\rangle + \frac{\mathcal{N}_-^2}{2\mathcal{N}_2}|-\rangle|-\rangle. \tag{22}$$

It is easy to show that $\mathcal{N}_- \to 0$ when $\gamma \to 0$. This accords with the formula for negativity $\mathcal{E}(\mathrm{ECS}_2) = \tanh(2\gamma^2)$ [36] that gives $\mathcal{E}(\mathrm{ECS}_2) = 0$ for $\gamma = 0$. For any nonzero γ the system in the state $|\mathrm{ECS}_2\rangle$ is entangled, and the negativity $\mathcal{E}$ rapidly reaches its the maximum value 1 when γ increases. Interestingly, when $\gamma > 1.3$ (i.e. $\mathcal{E}(\mathrm{ECS}_2) > 0.998$) the probability $\mathcal{P}_V$ of violation for ECS2 becomes similar to that for ECS1, including the formation of local minimum (figure 2).

(d) For the hybrid qubit-Schrödinger cat state the correlation function is derived as

$$C(\theta_a,\phi_a,\theta_b,\phi_b) = -\sin\theta_a\cos\phi_a\cos\theta_b + f_4(\gamma)\sin\theta_b(\cos\theta_a\cos\phi_b + \sin\theta_a\sin\phi_a\sin\phi_b), \tag{23}$$

where

$$f_4(\gamma) = \exp(-\gamma^2)\sum_{n=0}^{\infty}\frac{\gamma^{4n+1}}{\sqrt{(2n)!\,(2n+1)!}}. \tag{24}$$

As documented in figure 2, the probability $\mathcal{P}_V$ of violation for the hybrid state considered as a function of γ behaves similarly to that for ECS2 and forms a local minimum around $\gamma \approx 1.5$. For $\gamma \to 0$ the probability $\mathcal{P}_V$ of violation vanishes because the hybrid qubit-Schrödinger cat state is separable ($\mathcal{E}(H) = \sqrt{1-\exp(-4\gamma^2)}$). With the increasing amplitude $\gamma\mathcal{P}_V$ grows rapidly exceeding the values for ECS2 in the entire range of γ. This is a consequence of the relation $\mathcal{E}(H) \geqslant \mathcal{E}(\mathrm{ECS}_2)$ for any γ. This means that, for fixed γ, the hybrid qubit-Schrödinger cat state gets more entangled than the triplet-like ECS2.

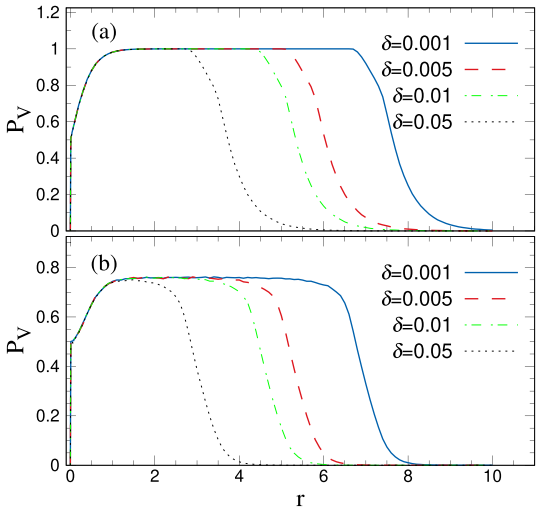

Figure 3. Probability $\mathcal{P}_{\mathrm{V}}$ of violation for the TMSS as a function of squeezing parameter r for the generalized BW scenario; the measurement parameters are sampled over (a) the real and (b) the whole complex planes.

3.2. Wigner-function formalism

Now we discuss the probability of violation $\mathcal{P}_{\mathrm{V}}$ analyzed for the Bell inequality expressed in terms of the Wigner function. In this case, the space of measurement parameters Ω is determined by four complex amplitudes α, α', β, and β' that are supposed to be sampled varying uniformly their real and imaginary parts in the range $(-\infty, \infty)$. However, this results in the trivial solution $\mathcal{P}_{\mathrm{V}} = 0$. To arrive at nonzero $\mathcal{P}_{\mathrm{V}}$, we have to restrict our sampling to a finite regime $\langle -\delta, \delta \rangle$. This accords with possible experimental realization. Namely, the displacement operation can be experimentally reached by combining a considered field with a highly excited coherent reference field $|z\rangle$ at a highly asymmetric beam splitter with transmission $T \approx 1$ [37, 38]. At the beam-splitter output, one gets a state displaced by the coherent amplitude $\alpha = -\mathrm{i}z\sqrt{1-T}$, i.e. the displacement operation $\hat{D}(\alpha)$ is realized on the input state (see [37] for details). It holds for fixed z that the greater the asymmetry $(1 - T \to 0)$ is, the smaller the amplitude α is. In the limiting case, $T = 1$ implies $\alpha = 0$. In our probabilistic scheme, it is not necessary to control the values of z and T when estimating $\mathcal{P}_{\mathrm{V}}$, which significantly reduces the experimental requirements. On the other hand, the limitation of the range of the parameters has an interesting physical interpretation, which will be discussed later, as it represents the uncertainty in experimental settings. Calculations made for different values of δ demonstrate the influence of uncertainty in setting the displacement parameters on testing the Bell inequalities.

The numerical calculations revealed the following results:

(a) The Wigner function for TMSS is obtained as [39]

$$W_{\mathrm{TMSS}}(\alpha, \beta) = \frac{4}{\pi^2} \exp[-2\cosh(2r)\left(|\alpha|^2 + |\beta|^2\right) + 2\sinh(2r)\left(\alpha\beta + \alpha^*\beta^*\right)]. \tag{25}$$

It is used to calculate the Bell function $\mathcal{B}_W$ given in equation (9). We first assume the BW scenario in which two of the four parameters are equal to zero ($\alpha = \beta = 0$). In this case, the probability $\mathcal{P}_{\mathrm{V}}$ of violation increases rapidly as the squeezing parameter r grows, and then the constant behavior characterized by $\mathcal{P}_{\mathrm{V}} = 1$ [0.76] for the measurement parameters sampled over the real [complex] values, as shown in figure 3(a) [(b)]. This means that, within the BW scenario, nonlocal correlations and thus entanglement of TMSS is detected for random settings with certainty provided that the amplitudes α' and β' are considered as real. This is a rather unexpected result as the Bell parameter $\mathcal{B}_W$ for TMSS violates the CHSH inequality much weaker compared to when the pseudospin formalism is applied [26]. For sufficiently high values of r the probability $\mathcal{P}_{\mathrm{V}}$ of violation is zero. The width of the constant behavior of $\mathcal{P}_{\mathrm{V}}$ strongly depends on the value of δ: The smaller the value of δ is, the greater the value of r is reached such that $\mathcal{P}_{\mathrm{V}} > 0$. From the experimental point of view, $\delta = 0.05$ appears to be sufficient for the current state-of-the-art experiments exhibiting squeezing around 15 dB ($r = 1.73$) [40].

A similar behavior of $\mathcal{P}_{\mathrm{V}}$ is observed when the generalized BW scenario is applied by randomly selecting all for measurement amplitudes. The difference is in the width of the constant behavior and the reached value of $\mathcal{P}_{\mathrm{V}}$ (see figure 4). In the generalized BW scenario, the maximal values of probability $\mathcal{P}_{\mathrm{V}}$ of violation reach 0.7 (0.38) when sampling over the real (complex) measurement amplitudes.

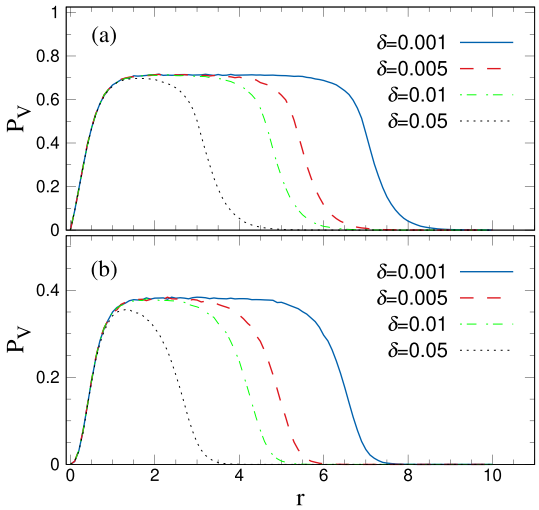

Figure 4. Probability $\mathcal{P}_{\mathrm{V}}$ of violation for the TMSS as a function of squeezing parameter r for the generalized BW scenario; the measurement parameters are sampled over (a) the real and (b) the whole complex planes.

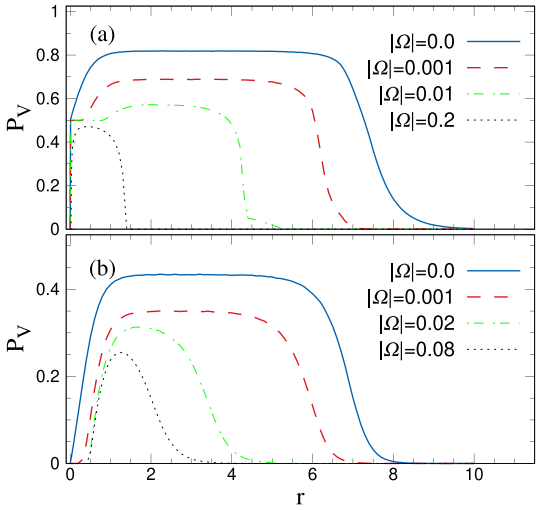

Figure 5. Probability $\mathcal{P}_{\mathrm{V}}$ of violation for the TMSS as a function of squeezing parameter r for the ring ($|\Omega| = 0$) and disc ($|\Omega| \neq 0$) sampling areas assuming $\delta = 0.001$. In (a) [(b)] [generalized] BW formalism is applied.

Let us reformulate the above results in a form better applicable to the real experimental situation in which the displacement amplitudes are generated with well-defined amplitudes but random phases. We thus assume that $\alpha = |\alpha| \exp(\mathrm{i}\phi_\alpha)$, where $|\alpha|$ [ϕ_α is uniformly distributed in the interval $\langle |\alpha|, |\alpha| + \delta \rangle$ [$\phi_\alpha \in \langle 0, 2\pi \rangle$]. The amplitudes α', β, and β' are defined similarly. The change in sampling geometry naturally affects the obtained results, as it follows from the comparison of curves in figure 5 with those plotted in figures 3 and 4. For the circular geometry, the probability $\mathcal{P}_{\mathrm{V}}$ of violation reaches noticeably higher values and drops down for larger r compared to the above-analyzed square geometry. With the increasing values of measurement amplitudes $|\alpha|, \ldots, |\beta'|$ the values of $\mathcal{P}_{\mathrm{V}}$ decrease for both methods. This confirms the conclusion that the probability $\mathcal{P}_{\mathrm{V}}$ of violation is very useful for experimental detection of nonlocal correlations, provided that the measurement amplitudes are small.

(b) For the singlet-like state ECS1, the Wigner function is given as [26]

$$\begin{aligned} W_{\mathrm{ECS}_1}(\alpha,\beta) = \frac{4}{\mathcal{N}_1 \pi^2} \Big(& \exp\left[-2\left(|\alpha|^2 + |\beta|^2 - 2\gamma \mathrm{Re}\{\alpha - \beta\} + 2\gamma^2\right)\right] \\ & + \exp\left[-2\left(|\alpha|^2 + |\beta|^2 + 2\gamma \mathrm{Re}\{\alpha - \beta\} + 2\gamma^2\right)\right] \\ & - \exp\left[-2\left(|\alpha|^2 + |\beta|^2 + 2\mathrm{i}\gamma \mathrm{Im}\{\alpha - \beta\}\right)\right] \\ & - \exp\left[-2\left(|\alpha|^2 + |\beta|^2 - 2\mathrm{i}\gamma \mathrm{Im}\{\alpha - \beta\}\right)\right] \Big). \end{aligned} \tag{26}$$

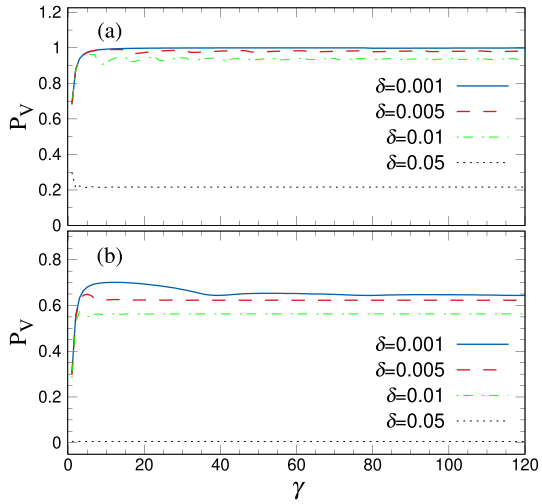

Figure 6. Probability $\mathcal{P}_V$ of violation for the state ECS1 as a function of coherent amplitude γ considering (a) [(b)] [generalized] BW scenario and complex amplitudes.

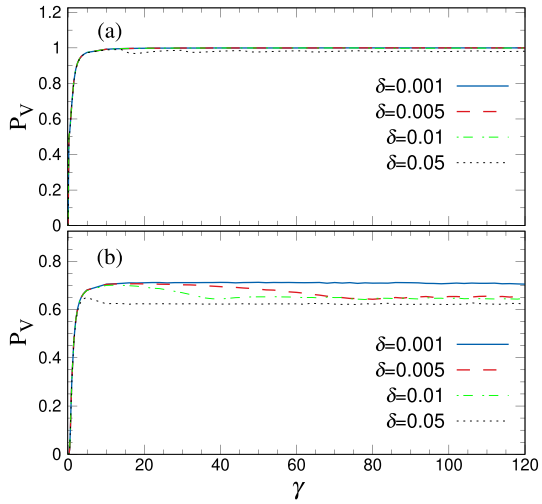

Figure 7. Probability $\mathcal{P}_V$ of violation for the state ECS2 as a function of coherent amplitude γ considering (a) [(b)] [generalized] BW scenario and complex amplitudes.

On the other hand, we get the Wigner function of the triplet-like state ECS2 in the form

$$\begin{aligned} W_{\mathrm{ECS}_2}(\alpha,\beta) = \frac{4}{\mathcal{N}_2\pi^2}\Big(&\exp\left[-2\left(|\alpha|^2+|\beta|^2-2\gamma\mathrm{Re}\left\{\alpha-\beta\right\}+2\gamma^2\right)\right] \\ &+\exp\left[-2\left(|\alpha|^2+|\beta|^2+2\gamma\mathrm{Re}\left\{\alpha-\beta\right\}+2\gamma^2\right)\right] \\ &+\exp\left[-2\left(|\alpha|^2+|\beta|^2+2\mathrm{i}\gamma\mathrm{Im}\left\{\alpha-\beta\right\}\right)\right] \\ &+\exp\left[-2\left(|\alpha|^2+|\beta|^2-2\mathrm{i}\gamma\mathrm{Im}\left\{\alpha-\beta\right\}\right)\right]\Big). \end{aligned} \tag{27}$$

As documented in figures 6 and 7, the probability $\mathcal{P}_V$ of violation grows rapidly with the increasing amplitude γ for both types of states and then it remains constant. It reaches the values around 0.98 (0.999) for ECS1 (ECS2) when $\gamma = 5$ assuming BW approach with $\delta = 0.001$. As the sampling range described by δ increases, the maximum achievable values of $\mathcal{P}_V$ decrease, especially for ECS1.

The generalized BW approach provides similar results as the BW approach, only the attainable values of $\mathcal{P}_V$ are smaller [compare the curves in figure 6(b) with those in figure 6(a) and also the curves in figure 7(b) with those in figure 7(a)].

Thus the BW approach is superior above the generalized BW approach and it allows to detect nonlocal correlations with randomly set measurement amplitudes in the entire range of γ. From this point of view, it is much more efficient than the pseudospin approach.

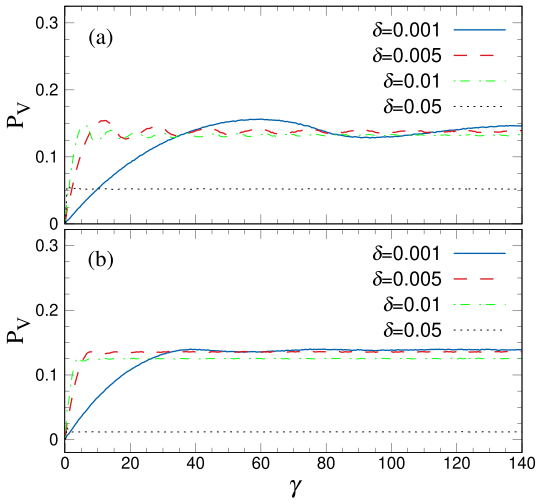

Figure 8. Probability $\mathcal{P}_{\mathrm{V}}$ of violation for the state HS as a function of coherent amplitude γ considering (a) [(b)] [generalized] BW scenario and complex amplitudes.

(c) For the hybrid state HS the above conclusions do not apply. Its Wigner function is determined in the form [41]

$$W_H(\phi,\theta,\beta) = \frac{1}{2\pi}\exp\left[-2|\beta-\alpha|^2\right]\left(1-\sqrt{3}\cos(2\theta)\right) + \frac{1}{2\pi}\exp\left[-2|\beta+\alpha|^2\right]\left(1+\sqrt{3}\cos(2\theta)\right) + \frac{\sqrt{3}}{\pi}\exp\left[-2|\beta|^2\right]\sin(2\theta)\cos\left(2\left(\phi+2\mathrm{Im}\left\{\beta\alpha^*\right\}\right)\right). \tag{28}$$

The values of probability $\mathcal{P}_{\mathrm{V}}$ of violation, determined by equation (13), lie below 0.2, as evidenced in figure 8. This means that they are considerably smaller than the values of $\mathcal{P}_{\mathrm{V}}$ reached in the pseudospin approach.

4. Conclusions

We have investigated the probability of violation of the CHSH inequalities under random measurements considering the probability as an indicator of nonlocal correlations. Contrary to the current literature devoted to discrete systems, we have analyzed specific continuous-variable and hybrid states. We have investigated the violation of the Bell inequality based on dichotomic observables using the pseudospin and the Wigner-function formalisms.

The pseudospin operator can be understood as the limiting case of the Gisin–Peres observable, ensuring the maximal violation of the CHSH inequality for the original Einstein–Podolsky–Rosen (EPR) state. In contrast, the original EPR state cannot maximally violate the CHSH inequality within the Banaszek–Woodkiewicz formalism or even its generalization that uses the Wigner function. However, the investigations of nonlocality based on the Wigner function are very important because of their realistic practical experimental realizations.

Our results have revealed that the Banaszek–Woodkiewicz formalism based on the Wigner functions gives high probabilities of CHSH-inequality violation under random measurements, much higher than those achieved in the pseudospin formalism. Specifically, the probability reaches the value of 0.78 for the two-mode squeezed vacuum state. For the entangled coherent states the probabilities are even greater approaching 1. This contrasts with the probabilities for hybrid states that lie below 0.2. For the hybrid states, the pseudospin formalism is much more efficient.

Random sampling allows for much simpler experimental procedures for the detection of the Bell nonlocality: The detection devices do not need initial setting and calibration and also no apriori information about the form of the state density matrix is needed. In the sense that the measurement settings do not need to be tailored to the state being tested. Thus, our method can be applied in unstable experimental environments where the discussed requirements are difficult to reach. This opens the door for much simpler and thus more efficient detection of the Bell nonlocality.

Data availability statement

All data that support the findings of this study are included within the article (and any supplementary files).

Acknowledgments

J P acknowledges support by the project OP JAC CZ.02.01.01/00/22_008/0004596 of the Ministry of Education, Youth, and Sports of the Czech Republic.

References

[1] Bell J S 1964 *Physics* **1** 195
[2] Einstein A, Podolsky B and Rosen N 1935 *Phys. Rev.* **47** 777
[3] Aspect A 1999 *Nature* **398** 189
[4] Brunner N, Cavalcanti D, Pironio S, Scarani V and Wehner S 2014 *Rev. Mod. Phys.* **86** 419
[5] Ekert A K 1991 *Phys. Rev. Lett.* **67** 661
[6] Buhrman H, Cleve R, Massar S and de Wolf R 2010 *Rev. Mod. Phys.* **82** 665
[7] Pironio S *et al* 2010 *Nature* **464** 1021
[8] Acín A, Brunner N, Gisin N, Massar S, Pironio S and Scarani V 2007 *Phys. Rev. Lett.* **98** 230501
[9] Rabelo R, Ho M, Cavalcanti D, Brunner N and Scarani V 2011 *Phys. Rev. Lett.* **107** 050502
[10] Scarani V 2012 *Acta Phys. Slovaca* **62** 347
[11] Liang Y C, Rosset D, Bancal J D, Pütz G, Barnea T J and Gisin N 2015 *Phys. Rev. Lett.* **114** 190401
[12] Scarani V and Gisin N 2001 *J. Phys. A: Math. Gen.* A **34** 6043
[13] Liang Y C, Harrigan N, Bartlett S D and Rudolph T 2010 *Phys. Rev. Lett.* **104** 050401
[14] Wallman J J, Liang Y C and Bartlett S D 2011 *Phys. Rev.* A **83** 022110
[15] Fonseca E A and Parisio F 2015 *Phys. Rev.* A **92** 030101(R)
[16] de Rosier A, Gruca J, Parisio F, Vértesi T and Laskowski W 2017 *Phys. Rev.* A **96** 012101
[17] Barasiński A, Černoch A, Laskowski W, Lemr K, Vértesi T and Soubusta J 2021 *Quantum* **5** 430
[18] Lipinska V, Curchod F, Máttar A and Acín A 2018 *New J. Phys.* **20** 063043
[19] Barasiński A, Černoch A, Lemr K and Soubusta J 2020 *Phys. Rev.* A **101** 052109
[20] Jiráková K, Barasiński A, Černoch A, Lemr K and Soubusta J 2021 *Phys. Rev. Appl.* **16** 054042
[21] Chen Z B, Pan J W, Hou G and Zhang Y D 2002 *Phys. Rev. Lett.* **88** 040406
[22] Clauser J F, Horne M A, Shimony A and Holt R A 1969 *Phys. Rev. Lett.* **23** 880
[23] Banaszek K and Wódkiewicz K 1998 *Phys. Rev.* A **58** 4345–7
[24] Banaszek K and Wódkiewicz K 1999 *Phys. Rev. Lett.* **82** 2009–13
[25] Wilson D, Jeong H and Kim M S 2002 *J. Mod. Opt.* **49** 851–64
[26] Jeong H, Son W, Kim M S, Ahn D and Brukner C 2003 *Phys. Rev.* A **67** 012106
[27] Bondani M, Allevi A and Andreoni A 2010 *J. Opt. Soc. Am.* B **27** 333–337
[28] Harder G, Silberhorn C, Rehacek J, Hradil Z, Motka L, Stoklasa B and Sánchez-Soto L L 2016 *Phys. Rev. Lett.* **116** 133601
[29] Kalash M and Chekhova M V 2023 *Optica* **10** 1142
[30] Kuzmich A, Walmsley I A and Mandel L 2000 *Phys. Rev. Lett.* **85** 1349–53
[31] Masanes L 2003 *Quantum Inf. Comput.* **3** 345
[32] Peřina J 1991 *Quantum Statistics of Linear and Nonlinear Optical Phenomena* (Kluwer)
[33] Tilma T, Everitt M J, Samson J H, Munro W J and Nemoto K 2016 *Phys. Rev. Lett.* **117** 180401
[34] Pozniak M, Zyczkowski K and Kus M 1998 *J. Phys. A: Math. Gen.* **31** 1059
[35] Mandel L and Wolf E 1995 *Optical Coherence and Quantum Optics* (Cambridge University Press)
[36] Hill S and Wootters W K 1997 *Phys. Rev. Lett.* **78** 5022
[37] Paris M G 1996 *Phys. Lett.* A **217** 78–80
[38] Laiho K, Avenhaus M, Cassemiro K N and Silberhorn C 2009 *New J. Phys.* **11** 043012
[39] Barnett S and Knight P 1987 *J. Mod. Opt.* **34** 841–53
[40] Vahlbruch H, Mehmet M, Danzmann K and Schnabel R 2016 *Phys. Rev. Lett.* **117** 110801
[41] Arkhipov I, Barasiński A and Svozilík J 2018 *Sci. Rep.* **8** 16955